JOURNAL OF VIROLOGY, Jan. 2006, p. 252–261 Vol. 80, No. 1
0022-538X/06/$08.00+0 doi:10.1128/JVI.80.1.252–261.2006

Defective Assembly of Influenza A Virus due to a Mutation in the Polymerase Subunit PA

John F. Regan,[1] Yuying Liang,[2] and Tristram G. Parslow[2]*

BioMedical Sciences Graduate Program, University of California, San Francisco, California 94143,[1] and Department of Pathology and Laboratory Medicine, Emory University School of Medicine, Atlanta, Georgia 30322[2]

Received 23 June 2005/Accepted 10 October 2005

The RNA-dependent RNA polymerase of influenza A virus is composed of three subunits that together synthesize all viral mRNAs and also replicate the viral genomic RNA segments (vRNAs) through intermediates known as cRNAs. Here we describe functional characterization of 16 site-directed mutants of one polymerase subunit, termed PA. In accord with earlier studies, these mutants exhibited diverse, mainly quantitative impairments in expressing one or more classes of viral RNA, with associated infectivity defects of varying severity. One PA mutant, however, targeting residues 507 and 508, caused only modest perturbations of RNA expression yet completely eliminated the formation of plaque-forming virus. Polymerases incorporating this mutant, designated J10, proved capable of synthesizing translationally active mRNAs and of replicating diverse cRNA or vRNA templates at levels compatible with viral infectivity. Both the mutant protein and its RNA products were appropriately localized in the cytoplasm, where influenza virus assembly occurs. Nevertheless, J10 failed to generate infectious particles from cells in a plasmid-based influenza virus assembly assay, and hemagglutinating material from the supernatants of such cells contained little or no nuclease-resistant genomic RNA. These findings suggest that PA has a previously unrecognized role in assembly or release of influenza virus virions, perhaps influencing core structure or the packaging of vRNAs or other essential components into nascent influenza virus particles.

The influenza A virus encodes a heterotrimeric RNA-dependent RNA polymerase whose subunits are designated PB1, PB2, and PA. Localized in the nuclei of infected cells, this trimeric complex is essential for transcribing all virally encoded mRNAs and for replicating the eight negative-sense single-stranded RNA segments (vRNAs) that make up the viral genome. To carry out transcription, the polymerase endonucleolytically cleaves short, 5′-capped oligonucleotides from cellular mRNAs to be used as primers, which are then elongated using all but a few nucleotides from any given vRNA as a template. Replication, by contrast, is achieved through a primer-independent, two-step process in which the polymerase first copies a vRNA template to produce a full-length cRNA and then uses this cRNA as the template for new vRNA synthesis.

Although all three polymerase subunits are required for viral infectivity, each of the known substrate-binding or catalytic activities of the complex appears to reside primarily in either the PB1 or PB2 subunit. The precise functions of PA are less certain. PA is 716 amino acids long and differs from the other two subunits in having an overall negative charge. Mutational studies from several laboratories have begun to delineate the functional architecture of PA and its roles in the influenza virus life cycle. Sequences near its N terminus (within residues 124 to 246) have been found to target PA into nuclei (21), whereas C-terminal residues 668 to 692 mediate its incorporation into the polymerase trimer by interacting specifically with PB1 (22, 26). Early studies of a temperature-sensitive mutation, later mapped to residue 226, indicated that PA might be specifically required for replication but not for transcription (10, 12). Mutation of residue 510, on the other hand, impairs transcription by decreasing cap-endonuclease activity, and point substitutions at a variety of other locations can diminish or eliminate synthesis of all three classes of viral RNA (3). Mutation of residue 638 has been found to promote synthesis and packaging of truncated, defective-interfering RNAs (4), perhaps reflecting impaired stability or processivity of the mutant polymerase complex. Collectively, these and other results suggest that PA may modulate or regulate diverse aspects of polymerase function. In addition, some reports have suggested that PA either possesses intrinsic proteolytic activity (7) or can induce generalized activation of cellular proteases (9, 25, 29), but contradictory findings have been reported (3, 18), and the possible relationship of proteolysis to polymerase function or viral growth remains unclear.

Here we report additional systematic mutagenesis aimed at better characterizing the roles of PA in influenza virus biology. We have constructed 16 novel PA mutants containing paired alanine substitutions that target conserved, polar residues along the entire length of the protein. Each of these mutants has been characterized with respect to its ability to support viral infectivity and the expression of viral RNAs and protein. Our results confirm and extend earlier work in indicating that PA mutations can yield a spectrum of effects on polymerase function. Additionally, however, we identify a novel mutation in PA that supports robust expression of all three classes of influenza virus RNAs, yet completely abolishes production of infectious viral particles. Our results are the first to suggest that PA plays an indispensable role in influenza virus virion assembly that is independent of RNA polymerase activity.

* Corresponding author. Mailing address: Department of Pathology and Laboratory Medicine, Emory University, 1364 Clifton Road NE, Room H-184, Atlanta, GA 30322. Phone: (404) 727-8657. Fax: (404) 727-3133. E-mail: tparslo@emory.edu.

TABLE 1. Properties of influenza viruslike particles containing WT or mutant PA proteins

Virus	Mutation(s)	Hemagglutination titer	Plaque titer	Plaque morphology[a]	Relative infectivity[b]
WT		64	1.0E + 07	Normal, clear	+++
J1	G81A, R82A	16	2.2E + 03	Small, turbid	+
J2	D111A, Y112A	16	0	NV	−
J3	E165A, E166A	16	0	NV	−
J4	M249A, S250A	16	5.0E + 04	Small, clear	+
J5	E351A, E352A	32	1.0E + 07	Normal, clear	+++
J6	K362A, T363A	16	8.0E + 05	Normal, clear	++
J7	R442A, R443A	16	0	NV	−
J8	Y445A, F446A	16	6.5E + 02	Small, clear	+
J9	E493A, G494A	16	5.0E + 06	Normal, clear	+++
J10	G507A, R508A	16	0	NV	−
J11	D514A, T515A	16	7.0E + 05	Small, turbid	++
J12	P530A, R531A	16	3.0E + 04	Small, turbid	+
J13	K536A, W537A	8	0	NV	−
J14	M579A, E580A	16	4.0E + 05	Small, clear	++
J15	S600A, S601A	64	1.0E + 06	Normal, clear	+++
J16	E656A, G657A	16	0	NV	−

[a] NV, none visible.
[b] Plaque-forming titers expressed as follows: +++, $>10^6$ PFU/ml; ++, 10^5 to 10^6 PFU/ml; +, $<10^5$ PFU/ml; −, no plaques visible.

MATERIALS AND METHODS

Plasmid construction and mutagenesis. The 17-plasmid influenza virus reconstitution system of Kawaoka and colleagues was used as described previously (19), except that the PA protein expression vector was modified to express coding sequences from the A/WSN/33 strain, identical to those in the PA vRNA vector. The substitution mutations listed in Table 1 were first introduced into the PA vRNA vector through PCR-based mutagenesis and then subcloned into the PA protein vector using unique ClaI and ApaI restriction enzyme sites and verified by sequencing. This strategy inserted a truncated human RNA polymerase I promoter at the C-terminal end of every mutant or wild-type (WT) PA protein vector used in this study.

To create luciferase-encoding reporters, the luciferase gene from pGL3 (Promega) was amplified by PCR using primers that added the 3′ or 5′ untranslated region from the neuraminidase (NA) vRNA or cRNA onto each end, flanked by BsmBI sites; the products were then inserted into the BsmBI site of the vector pHH21 (8, 19). The PB2-GFP reporter vector, encoding a fusion of 151 N-terminal residues from PB2 to the N terminus of green fluorescent protein (GFP), has been described elsewhere (15). The NS-GFP reporter, which encoded 79 N-terminal residues of influenza virus NS1 protein fused to the N terminus of GFP, was created by replacing a unique NcoI-MfeI fragment from the coding region in the NS protein expression vector with a GFP cassette.

Cells and antibodies. 293T, MDBK, and MDCK cells were maintained as described previously (1, 19). Anti-PA polyclonal antibodies were obtained by immunizing rabbits against a recombinant protein comprising 204 N-terminal residues of PA from strain WSN/33 with a six-His C-terminal tag. Other primary antibodies included mouse anti-M1 (Serotec), mouse antinucleoprotein (anti-NP) (Serotec), rabbit anti-GFP, mouse antimitochondria (Ab-2; Lab Vision), and rabbit anti-histone H3 (Novus Biologicals). Secondary antibodies used for Western blotting were goat anti-mouse immunoglobulin G and donkey anti-rabbit immunoglobulin G, both peroxidase conjugated (ImmunoPure; Pierce Endogen).

Transfections and expression assays. 293T cells were transfected transiently on 35-mm plates using TransIT-LT1 (Mirus). For viruslike particle (VLP) production by 17-plasmid transfection, cells were transfected as described previously (19), with vector additions or substitutions as indicated. To assay polymerase function by five-plasmid transfection, cells were transfected with 1 μg each of an indicated reporter and of the protein expression vectors encoding PB2, PB1, PA, and NP. A β-galactosidase (β-Gal) expression plasmid, pCH110 (Pharmacia), was included in some studies as an internal control for normalizing transfection efficiency. At indicated times, cells were harvested either for luciferase assay or for isolation of total cellular RNA using Trizol (Invitrogen). The luciferase assay was conducted according to the manufacturer's protocol (Promega) using a Turner Designs 20/20 luminometer, after normalization to β-Gal activity.

Primer extension assays. Primers were ^{32}P end labeled with T4 polynucleotide kinase (Invitrogen) and designed to bind near the 5′ ends of RNA species. First-strand cDNA synthesis was carried out as described by Fodor et al. (3), and the products were analyzed by electrophoresis on a 6% polyacrylamide-urea gel. The predicted sizes of the ^{32}P-labeled cDNA products are listed below, in parentheses, after each primer sequence.

When detecting RNA generated from pol NA-Luc reporters the following primers were used: vLuc75, 5′-GAGAGATCCTCATAAAGGC-3′ (vRNA, 75 nucleotides [nt]), and cLuc84, 5′-GCGGTTCCATCTTCCAGCGG-3′ (cRNA, 84 nt, and mRNA, 93 to 96 nt). When detecting RNA generated from the pol NS 238-GFP-374 reporter, the following primers were used: vNS145, 5′-TGAGAC ACAGACTGAAGATAACAGA-3′ (vRNA, 145 nt), and cNS105, 5′-GTTCTT GGTCTGCAACTCTTTTGCG-3′ (cRNA, 105 nt, and mRNA, 114 to 118 nt). To detect native NA viral RNA species, the following primers were used: vNA155, 5′-GGGGCTACCTGAGGAGGACGCA-3′ (vRNA, 155 nt), and cNA125, 5′-GGCTAATCCATATTGAGATTATATT-3′ (cRNA, 125 nt, and mRNA, 134 to 138 nt).

Isolation of VLPs and infection of MDCK cells. Transfection supernatants were clarified of debris by centrifugation at 2,000 rpm for 10 min and then further purified by ultracentrifugation at 27,700 rpm for 3 h through a 20% sucrose cushion. Pellets were resuspended in phosphate-buffered saline and assayed for viral M1 protein by Western blotting. Aliquots containing equivalent amounts of M1 were then used to infect MDBK or MDCK cells; the approximate multiplicity of infection for wild-type VLPs was 2.2. Plaque-forming titer was estimated by serial 10-fold dilutions on MDCK monolayers as a measure of infectivity.

Quantitative reverse transcriptase PCR (RT-PCR). First-strand cDNA was synthesized from RNA samples using Superscript III RNase H$^-$ reverse transcriptase (Invitrogen) and then quantified with the specific forward (F) and reverse (R) primer pairs listed below. Quantitative PCR was performed using an ABI Prism 7700 sequence detector (Applied Biosystems).

The primer pairs and probes used to amplify and quantify viral sequences included PB2-F, 5′-ACGTGGTGTTGGTAATGAAACG-3′; PB2-R, 5′-TGG CCATCCGAATTCTTTTG-3′; cPB2-FAM, 6FAM-CGGAACTCTAGCATA CTTACTGACAGCCAGACA-TAMRA; PB1-F, 5′-GAATCTGGAAGGATA AAGAAAGAGGA-3′; PB1-R, 5′-CACTATTTTTGCCGTCTGAGCTC-3′; cPB1-VIC, VIC-TTCACTGAGATCATGAAGATCTGTTCCACCA-TAMRA; PA-F, 5′-TTAATGATCCCTGGGTTTTGCT-3′; PA-R, 5′-TTGCCACAACTA TCTCAATGCAT-3′; cPA-FAM, 6FAM-AATGCTTCTTGGTTCAACTCC TTCCTCACA-TAMRA; HA-F, 5′-TCAGATTCTGGCGATCTACTCAAC T-3′; HA-R, 5′-TAGAACACATCCAGAAACTGATTGC-3′; cHA-VIC, VIC-TCACTGGTGCTTTTGGTCTCCCTGG-TAMRA; NA-F, 5′-TGTCAA TGGTGAACGGCAACT-3′; NA-R, 5′-TCTTTTTGTGGTGTGAATAGT GATACTG-3′; vNA-FAM, 6FAM-AGCACCGTCTGGCCAAGACCAATC-TAMRA; NP-F, 5′-CGGACGAAAAGGCAACGA-3′; NP-R, 5′-CATTGT CTCCGAAGAAATAAGATCCT-3′; cNP-VIC, VIC-CGATCGTGCCCTCCT TTGACATGAGT-TAMRA; M-F, 5′-CTATGTTGACAAAATGACCAT CGTC-3′; M-R, 5′-TGCCAGAGTCTATGAGGGAAGAAT-3′; vM-FAM, 6FAM-CCACAGCATTCTGCTGTTCCTTTCGA-TAMRA; NS-F, 5′-CAA TAGTTGTAAGGCTTGCATAAATGTT-3′; NS-R, 5′-GAAGAAATAAGA

TGGTTGATTGAAGAAG-3′; and vNS-VIC, VIC-TTGCTCAAAACTATT CTCTGTTATCTTCAGTCTGTGTCTC-TAMRA (Invitrogen). Viral RNAs in cellular extracts were assayed after normalization for expression of the cellular 5.8S rRNA, which was detected using 5.8S-F, 5′-TAGCCCCGGGAGGAACC-3′; 5.8S-R, 5′-AGCGCTAGCTGCGAGAATTAA-3′; and v5.8S-VIC, VIC-TGT CGATGATCAATGTGTCCTGCAATTCAC-TAMRA.

Fluorescence-activated cell sorting analysis. Two-color flow cytometric analysis of transfected 293T cells or infected MDBK cells was conducted as described by Liang et al. (15). Sorting of cells was performed using a MoFlo instrument (Dako Cytomation).

Isolation of nuclear and cytoplasmic fractions. 293T cells were lysed for 5 min on ice in a hypotonic sucrose buffer (320 mM sucrose, 5 mM $MgCl_2$, 10 mM HEPES, pH 7.4) supplemented with 1% (vol/vol) Triton X-100. Nuclei were separated from cytoplasm by centrifugation at 2,000 × *g* for 1 min and then were washed twice in the sucrose buffer minus Triton X-100 and resuspended in the sucrose buffer.

Gradient centrifugation. VLPs were filtered through 0.45-μm polyethersulfone membrane filters (Whatman) and then pelleted through a 30% glycerol cushion by centrifugation at 25,000 rpm for 3 h in an SW-41 Ti rotor at 4°C. Pellets were resuspended and layered over 30 to 50% continuous glycerol gradients and again centrifuged in the same rotor at 25,000 rpm for 2 h at 4°C. Fractions were collected from the bottom, assayed for plaque-forming titer, and then concentrated by centrifugation through a 30% cushion as before. Pellets were resuspended in phosphate-buffered saline.

Agglutination of chicken erythrocytes. VLPs were incubated with 200 μl of glutaraldehyde-stabilized chicken red blood cells (Research Diagnostics, Inc.) with agitation for 1 h at 4°C. The cells were washed three times with Opti-MEM buffer supplemented with 0.3% (wt/vol) bovine serum albumin and 0.01% (vol/vol) fetal bovine serum and then treated with 600 units of micrococcal nuclease (MCN) for 1 h at 37°C. RNA was harvested from the samples with the QIAamp viral RNA minikit (QIAGEN) and assayed by quantitative RT-PCR and primer extension assays.

RESULTS

These studies utilized a reverse-genetic system (19) comprising 17 plasmid expression vectors that together encode the eight wild-type vRNAs and all essential viral proteins of influenza A virus. When transfected transiently into 293T cells, these 17 plasmids direct the assembly and release of infectious influenza virus particles that can subsequently be passaged indefinitely. In this report, we refer to the products of an initial transfection as VLPs, whereas any particles that have been passaged one or more times are termed virions, regardless of their origin. The 17-plasmid system used here includes two vectors that encode the PA protein and PA vRNA, respectively, each derived from the A/WSN/33 strain. We created mutations, designated J1 to J16, that each replaced two consecutive codons in the PA coding sequence with alanine codons; identical mutations were introduced into both the vRNA and protein expression vectors. These mutations, shown schematically in Fig. 1A and listed in Table 1, generally targeted residues that were hydrophilic, likely to be exposed on the protein surface, and evolutionarily conserved.

The wild-type and mutant PA protein expression vectors, along with a β-Gal expression vector as internal control, were each transfected into 293T cells, which were then lysed 22 h later and assayed for PA protein by Western blotting. As shown in Fig. 1B, all 16 mutants were of the expected relative mobility and were expressed at steady-state levels approximating that of the wild-type protein when normalized to β-Gal activity.

We initially surveyed the functional effects of these mutations in the 17-plasmid reconstitution system. In these first experiments, 293T cells were transfected with a mutant PA vRNA together with wild-type forms of all other essential viral components, including wild-type PA protein; thus, wild-type PA was expressed in the transfectants, but any resulting VLPs could transduce only the mutant vRNA. Supernatants were harvested 48 h after transfection and were assayed for plaque-forming activity on MDCK cells. As summarized in Table 1, six of the mutants (J5, J6, J9, J11, J14, and J15) had titers above 10^5 PFU/ml, comparable to that seen with wild-type PA, though with various plaque morphologies. Mutants J2, J3, J7, J10, J13, and J16, by contrast, produced no plaques, while the four remaining mutants (J1, J4, J8, and J12) yielded markedly reduced but measurable titers (10^2 to 10^4 PFU/ml) and abnormally small plaques. In each instance where plaques were obtained, we harvested RNA from plaque-purified virus, amplified PA coding sequences by RT-PCR, and verified that the expected mutation was indeed present. Curiously, the J1 mutant reproducibly yielded plaques from the initial transfection supernatants but could not be plaque purified.

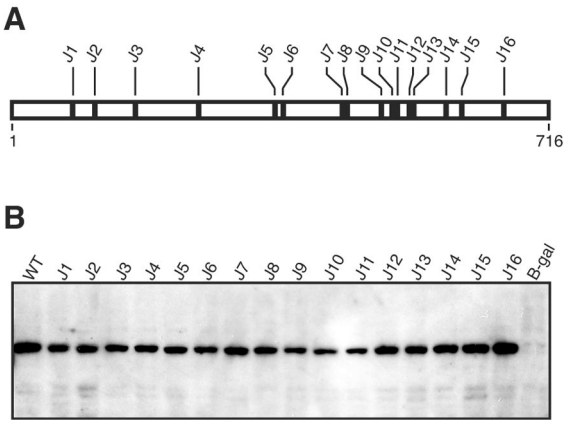

FIG. 1. Structure and expression of PA mutants. (A) Schematic depiction of mutations studied here, which were introduced into the PA protein of strain A/WSN/33. (B) Western blot detection of WT and mutant PA proteins in lysates of 293T cells transfected with the PA expression vector and a β-Gal control vector. Samples were normalized by β-Gal activity and analyzed using a polyclonal anti-PA antibody. β-Gal, cells transfected with the control vector alone.

To estimate the production and release of viral structural proteins, supernatants from the 17-plasmid transfections were also assayed for their ability to agglutinate chicken erythrocytes. The hemagglutination titers of the mutants, listed in Table 1, were generally two- to fourfold lower than that of the wild type and tended to be lowest for mutants that had very low plaque-forming activity. These modestly reduced hemagglutination titers likely reflect an inability of the most severely defective mutant polymerases to amplify viral protein expression by transcribing new viral mRNAs in the transfected cells (see below). Nevertheless, the observed differences in hemagglutination titer were not sufficient to account for the effects on PFU titer, which ranged over at least 7 orders of magnitude.

We next evaluated the ability of polymerases containing the various PA mutants to support viral RNA expression in cells. In these experiments, each transfection included only five viral expression plasmids. One was a reporter encoding a modified influenza virus NA vRNA in which a luciferase cassette (in the negative sense) replaced the native NA coding sequences. The other four directed expression of the viral PA, PB1, PB2, and

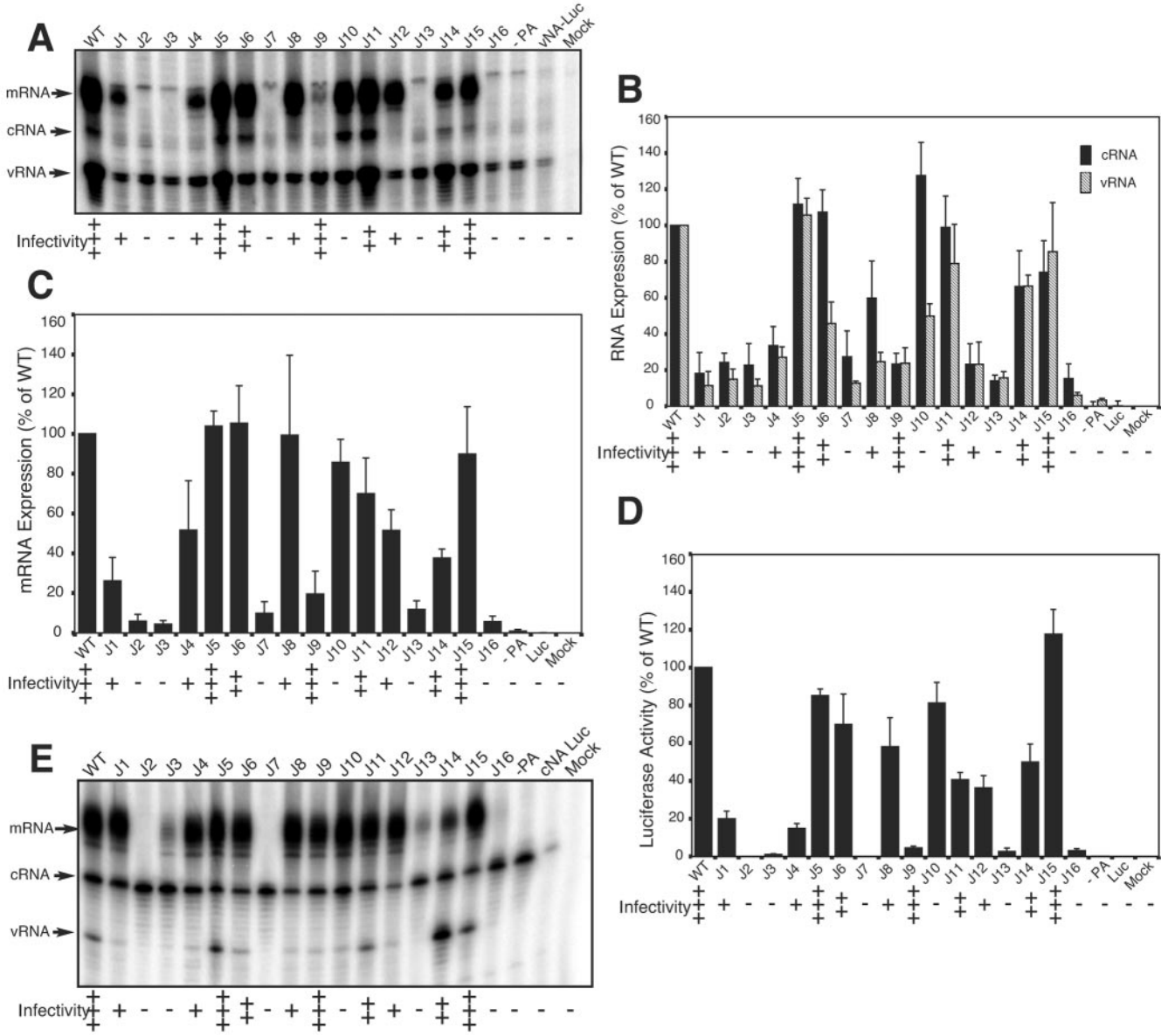

FIG. 2. Reporter RNA expression by mutant influenza virus polymerase in cells. 293T cells underwent five-plasmid transfections that included either the WT PA protein vector or the indicated mutants, along with a luciferase reporter vector representing either the vRNA (A to D) or cRNA (E) product of the influenza virus NA gene. Total RNA was harvested 36 h (for the vRNA reporter) or 44 h (for the cRNA reporter) after transfection and was probed for NA-specific vRNA, cRNA, and mRNA by primer extension assay. Representative products from the vRNA reporter are shown in panel A. Expression of each RNA type was quantified by phosphorimaging from three independent transfections; the relative amounts of cRNA (black bars) and vRNA (striped bars) are presented in panel B, and those of mRNA are shown in panel C, each relative to the corresponding WT. Luciferase expression from triplicate transfections is depicted in panel D. Representative products from the cRNA reporter are shown in panel E. Mock, sham-transfected cells. Luc, reporter plasmid (vRNA or cRNA) only. −PA, PA vector omitted. Relative infectivities of the PA mutants (from Table 1) are indicated at the bottom of each panel.

NP proteins, respectively, which together are known to be sufficient to support both replication and transcription from a vRNA template (24). We transfected 293T cells with those five plasmids, along with the β-Gal internal control vector; harvested RNA 36 h later; and quantified reporter-specific mRNA, cRNA, and vRNA sequences simultaneously using a primer extension assay. Representative results are depicted in Fig. 2A, and quantitative data from triplicate experiments are summarized for the individual RNA species in Fig. 2B and C. As expected, transfecting the reporter either alone (Luc) or in combination with only the PB1, PB2, and NP plasmids (−PA) revealed low-level background expression of reporter-derived vRNA that was undetectable in sham-treated cells (Mock). None of the latter control transfections yielded appreciable amounts of reporter cRNA or mRNA, however, confirming that PA is required for polymerase activity in this assay. By contrast, inclusion of the WT PA vector led to the synthesis of all three reporter-derived RNA species, with vRNA and

mRNA predominating, indicating the formation of a catalytically active polymerase. Through similar transfections in which various mutants replaced wild-type PA, we found that five mutants (J2, J3, J7, J13, and J16) yielded nonfunctional polymerases (Fig. 2A to C), a finding that accords with their complete inability to support viral infectivity (Table 1). Not surprisingly, five other mutants (J5, J6, J11, J14, and J15) that had previously demonstrated moderate or high infectivity each expressed at least 50% of the wild-type levels of vRNA, cRNA, and mRNA. Of note, J9 appeared less active, generating levels of all three RNA classes that were only 20 to 30% of wild-type levels, though it had yielded high-titer plaque-forming VLPs (Table 1). This implies that even mutants which function comparatively poorly in this five-plasmid assay may be compatible with full infectivity.

To verify that the mRNAs produced by these mutants were functional, extracts of cells from the five-plasmid transfections were also tested for luciferase activity using a luminescence assay (Fig. 2D). Comparison with Fig. 2C reveals that luciferase activity roughly corresponded to the level of reporter mRNA expressed by each mutant, implying that these mRNAs were biologically active. As a further test of polymerase integrity, we also created a positive-sense (cRNA) form of the NA-based luciferase reporter and tested the ability of each mutant to act on these cRNAs as substrates, using the five-plasmid assay. As shown in Fig. 2E, only modest steady-state yields of vRNA were obtained, generally from the highest-titer mutants (cf. Fig. 2A); nevertheless, the ability of mutants J1, J4 to J6, J8 to J12, J14, and J15 to produce abundant mRNA under these conditions implied production of a functional vRNA intermediate.

The most remarkable phenotype was that of J10, which supported robust expression of all three classes of reporter RNA (Fig. 2) yet consistently failed to produce plaque-forming virus (Table 1). For this mutant, vRNA, cRNA, and mRNA expression were 50% ± 7%, 128% ± 18%, and 86% ± 12%, respectively, of the wild-type levels in the five-plasmid luciferase vRNA reporter assay (Fig. 2B). Indeed, the expression levels of all three RNAs by J10 equaled or exceeded those obtained with other mutants (J4, J6, J8, J9, and J12) that produced infectious VLPs (Fig. 2B to D). Uniquely among our mutants, J10 thus appeared unable to support detectable viral infectivity despite generating a polymerase complex that was competent for both RNA replication and transcription. We therefore characterized the J10 mutant in greater detail.

We first used the 17-plasmid expression system to determine whether the failure of J10 supernatants to form plaques (Table 1) reflected a lack of viral RNA or protein synthesis in the MDCK target cells. In these and all subsequent experiments, transfected 293T cells received either wild-type or J10 forms of both the PA protein and vRNA vectors and so expressed exclusively wild-type or mutant PA. Supernatants from the transfectants were harvested after 48 h and used to infect MDCK cells, after normalization for viral matrix (M1) protein, a marker for virion particles which we found was roughly sevenfold more abundant in wild-type than J10 supernatants (data not shown). Extracts of the MDCK cells were then probed for M1 protein by Western blotting and for its corresponding RNAs by quantitative RT-PCR. We found that M1 protein was undetectable in cells immediately after exposure to wild-type VLPs but had

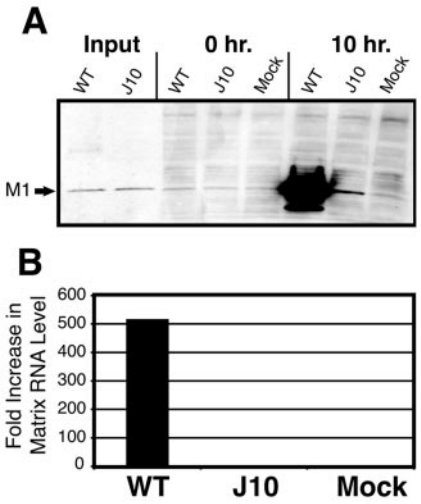

FIG. 3. Protein and RNA expression in infected MDCK cells. Aliquots of 293T supernatants from 17-plasmid transfections with WT or J10 PA vectors were normalized for influenza virus matrix (M1) protein expression and used to infect MDCK cells. (A) Western blot detection of M1 protein in 293T supernatants (Input) and in the MDCK cells at 0 h and 10 h postinfection. (B) Expression of M1-specific RNA as determined using quantitative RT-PCR, normalized to 5.8S rRNA, indicated as the fold increase at 5.5 h compared to 0 h postinfection. Mock, sham-infected MDCK cells.

accumulated in large amounts 10 h later, implying new synthesis (Fig. 3A). This was accompanied by a 500-fold accumulation of M1-specific RNA within 6 h after infection (Fig. 3B). Exposure to supernatants from J10 transfectants, by contrast, yielded little or no detectable synthesis of the viral M1 protein or its RNA.

Those results were extended by using a flow cytometric assay to count and characterize individual infected cells (15). In this assay, 293T cells were transfected with the 17-plasmid expression system along with a reporter derived from the PB2 vRNA that had been modified to encode GFP in antisense orientation. Supernatants were collected after 48 h, and aliquots were used to infect MDBK cells, which were harvested soon (15 h) after inoculation to avoid subsequent rounds of infection. Both the 293T producer and MDBK target cells were then fixed, permeabilized, and indirectly immunostained for viral NP, and 20,000 cells from each population were analyzed using two-color flow cytometry to detect GFP (green) and NP (red) expression. As shown in Fig. 4 (top left panel), roughly 17% of 293T cells transfected with all 17 wild-type vectors along with the reporter expressed NP protein alone, and an additional 15% of cells expressed both NP and GFP. By comparison, identical transfections using the J10 mutants of both the PA protein and vRNA vectors (top right panel) yielded a similar frequency of NP expression alone (16%), and only modestly lower (9%) dual expression of NP with GFP. Because GFP expression in this assay requires that the reporter vRNA first be transcribed into functional mRNA, this finding confirms that J10-containing polymerase is competent to transcribe vRNA. Moreover, when wild-type supernatants were used to infect MDBK cells (center left panel), roughly 90% of target cells acquired expression of NP, GFP, or both. Identical infections using J10 supernatants (center right panel), by contrast,

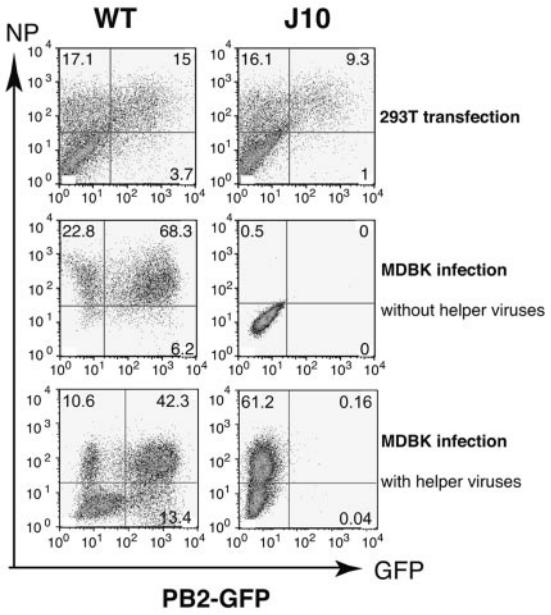

FIG. 4. Expression and transduction of influenza virus NP and of a vRNA-derived reporter in 293T producer and MDBK target cells. 293T cells underwent 17-plasmid transfections that included WT or J10 mutant PA vectors and a PB2-derived vRNA reporter vector that encoded GFP. Supernatants harvested after 48 h were used to infect MDCK cells. Two-color flow cytometry was used to score expression of immunoreactive NP protein and of GFP fluorescence in the 293T producer cells at 48 h posttransfection (top) and in the MDBK target cells at 15 h after inoculation with supernatant either alone (center) or together with authentic influenza virus helper virions at a multiplicity of infection of approximately 1.5 (bottom). Percentages of cells expressing NP only, GFP only, and the two markers together are indicated in the upper left, lower right, and upper right quadrants, respectively, of each plot, based on counting 20,000 cells from each population. As expression of the GFP reporter is assumed to require NP, the small percentage of cells expressing GFP alone was disregarded in our analysis. NP expression in the bottom right panel presumably results from infection with the helper virus.

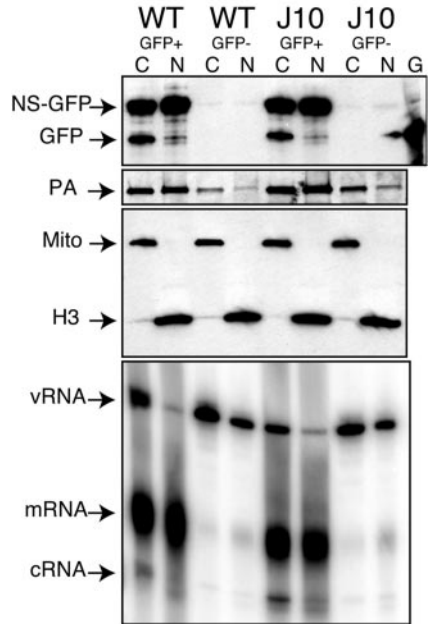

FIG. 5. Subcellular localization of viral RNAs and PA protein in 293T transfectants. 293T cells underwent five-plasmid transfection that included either the WT or J10 form of the PA protein vector, along with an NS-derived vRNA reporter encoding an NS1-GFP fusion protein. At 31 h posttransfection, cells were sorted into GFP-positive (GFP+) and GFP-negative (GFP−) subpopulations, from which nuclear (N) and cytoplasmic (C) extracts were then prepared. G, cells transfected with GFP reporter alone. Expression of the NS1-GFP fusion (NS-GFP), unfused GFP, PA, and histone H3 proteins, and of a mitochondrial antigen (Mito), was determined by Western blotting (top three panels). The vRNA, mRNA, and cRNA products of the NS vRNA reporter were detected by primer extension (bottom panel).

yielded virtually no cells expressing NP or GFP. Thus, despite supporting substantial polymerase activity in transfected 293T cells, the J10 mutant fails to generate VLPs that can detectably transduce native viral (NP) or reporter (GFP) vRNAs into other cells. Even when the J10 supernatant was supplemented with excess wild-type helper virions as a source of functional polymerase and NP, GFP expression remained undetectable (lower right panel), confirming the absence of transduction-competent VLPs.

One hypothetical explanation for this failure to transduce was that the vRNAs produced in J10-transfected cells might be inappropriately localized and hence unavailable at sites of virion assembly in the cytoplasm. To address this possibility, we transfected 293T cells with a vRNA reporter and the four protein vectors (PA, PB1, PB2, and NP) needed for polymerase function and then examined the distributions of selected RNAs and proteins in the nuclear and cytoplasmic compartments. The reporter was derived from the NS vRNA and encoded an in-frame fusion of the N-terminal 79 residues of influenza virus NS1 protein to the N terminus of GFP. Cells were harvested 30 h after transfection, and the WT and J10 populations were each physically sorted into GFP-expressing (GFP^+) and nonexpressing (GFP^-) subpopulations by fluorescence-activated cell sorting. We then prepared nuclear and cytoplasmic fractions from these four subpopulations and assayed selected proteins and RNAs in each (Fig. 5). The purity of the fractions was verified by Western blot detection of mitochondrial (Mito) and histone (H3) proteins that serve as markers of cytoplasm and nucleus, respectively. As expected, Western blotting revealed immunoreactive GFP only in the two GFP^+ subpopulations and so validated the sorting procedure. The NS-GFP fusion protein, which includes a nuclear localization signal from NS1 (6, 14), was distributed equally between nuclear and cytoplasmic compartments, whereas unfused GFP (resulting from translational initiation at the internal GFP start codon) was largely confined to the cytoplasm. Wild-type PA protein and the J10 mutant, detected using an antibody that recognizes both, were expressed at comparable levels in the nucleus and cytoplasm of GFP^+ cells and also (at somewhat lower abundance) in GFP^- cells, a proportion of which presumably expressed PA protein without the reporter or other polymerase subunits needed for GFP expression. Similarly, primer extension assay (bottom panel) revealed reporter-derived vRNA in the two GFP^- populations, with little or no accompanying mRNA or cRNA products to indicate polymerase activity. The GFP^+ cells, by contrast, showed abundant reporter mRNA in both cellular compartments, along with

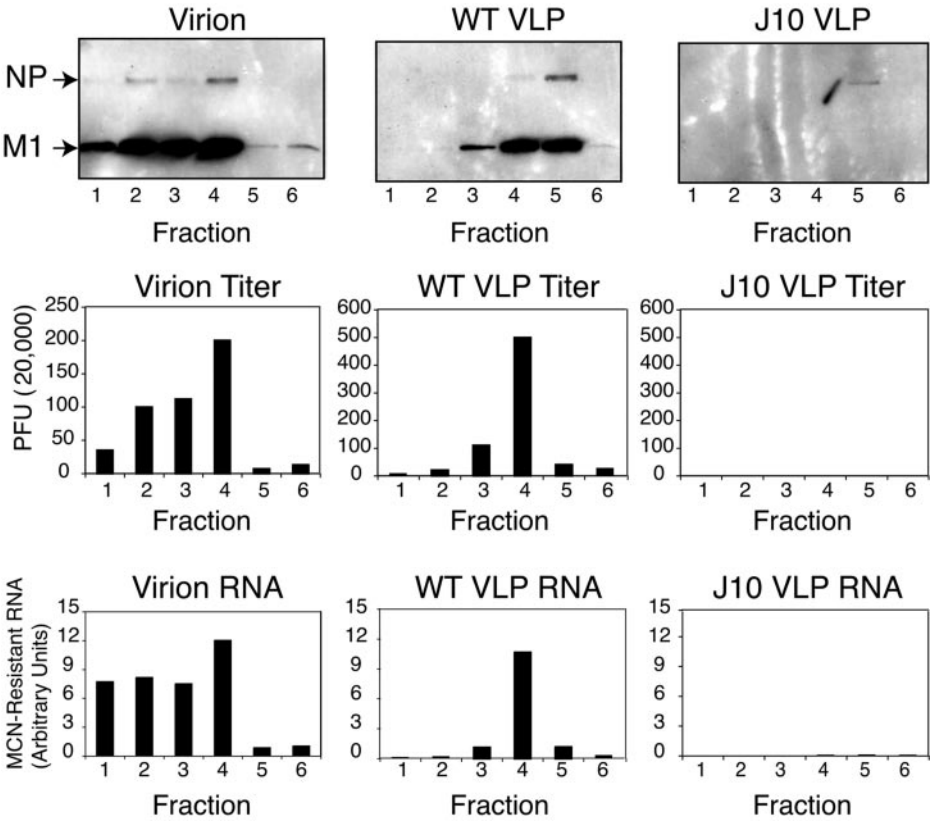

FIG. 6. Density gradient fractionation of virions and VLPs. Supernatants from 293T cells, collected 48 h after 17-plasmid transfection, were used as a source of WT or J10 VLPs. Supernatants from infected MDCK cells were used as a source of authentic influenza virus A/WSN/33 virions. These supernatants were fractionated by centrifugation through continuous glycerol density gradients, and corresponding fractions were analyzed for viral NP and matrix (M1) proteins by Western blotting (top panel), for plaque-forming activity (middle panel), and for MCN-resistant PB1-specific viral RNA by quantitative RT-PCR (bottom panel).

substantial vRNA and traces of cRNA that were each predominantly cytoplasmic. These localization patterns may differ somewhat from those seen in infected cells, owing to overexpression, absence of other viral proteins, or other attributes of the five-plasmid expression system. Nevertheless, it is clear from these results that expression and localization of all three classes of viral RNA, and of the PA protein itself, are comparable in cells transfected with either wild-type PA or J10. In particular, both forms of PA yielded similar amounts of PA protein and reporter vRNA in the cytoplasm, where virion assembly occurs.

To examine VLP formation, we analyzed supernatants from 17-plasmid 293T transfectants using density gradient centrifugation. Authentic influenza virus A/WSN/33 virions were analyzed in parallel for comparison. Each was fractionated through a linear glycerol gradient, and fractions were then assayed by Western blotting for the viral M1 and NP proteins (Fig. 6, top), by plaque-forming assay (middle), and by quantifying micrococcal nuclease-resistant viral RNA, a hallmark of virion particles (bottom). Authentic virions, containing both M1 and NP protein, sedimented in fractions 2 to 4, which also exhibited high levels of plaque-forming activity and of nuclease-resistant RNA. Supernatants from wild-type transfections likewise contained abundant VLPs with peak infectivity and RNA content localized in fraction 4, though M1 and NP immunoreactivities peaked at somewhat lower buoyant density in fraction 5, perhaps representing polymeric aggregates of those proteins without associated viral RNA (5, 28). Corresponding fractions from the J10 supernatants, by contrast, contained only traces of NP without associated M1 immunoreactivity or nuclease-resistant RNA and lacked any detectable plaque-forming activity. J10-transfected cells thus fail to generate VLPs whose density resembles that of wild-type VLPs or genuine influenza virus virions.

These gradient fractionation results did not, however, exclude the existence of J10-containing VLPs that were heterodisperse or anomalous in size, shape, and density. Expression of the viral M1, NA, and hemagglutinin proteins from their respective plasmid vectors should alone be sufficient to generate hemagglutinating VLPs even in the absence of polymerase function (13, 20), and this, together with cytolytic debris, could account for the high hemagglutinating titer that we observed in J10 supernatants (Table 1). As an alternative approach to enriching such VLPs, we therefore incubated 293T supernatants with chicken erythrocytes, which were then pelleted, washed, and probed for influenza virus proteins and vRNAs. Western blots (Fig. 7A) confirmed that the erythrocyte-adsorbed material from authentic virions (Vir) or from supernatants of cells transfected with the full complement of 17 WT vectors contained abundant M1 and PA proteins, but neither

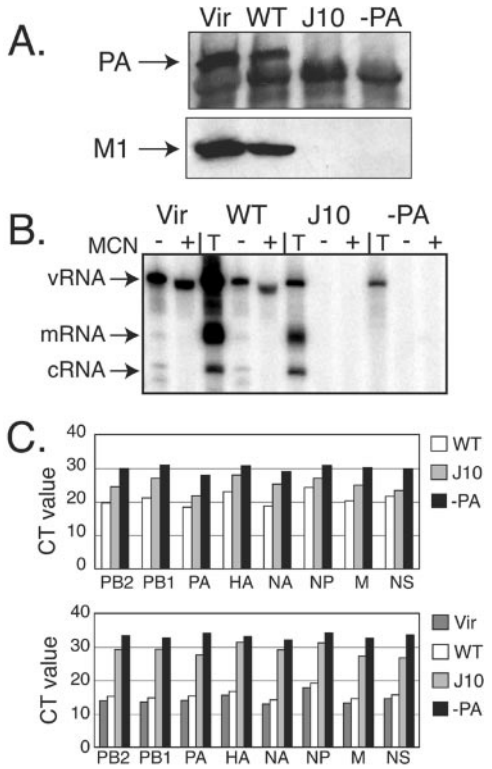

FIG. 7. Enrichment of hemagglutinating particles by adsorption to chicken erythrocytes. Supernatants from infected MDCK cells were incubated with chicken red blood cells to adsorb authentic influenza virus virions (Vir) and other hemagglutinating material. Similar adsorption was performed using supernatants from 17-plasmid 293T transfections that included WT or mutant (J10) PA vectors or from which PA vectors had been omitted (−PA). Erythrocytes were pelleted, washed, and then lysed for Western blot analysis. Alternatively, the washed erythrocyte pellets were incubated for 1 h at 37°C either with (+) or without (−) MCN, and RNA was then extracted for analysis, along with RNA from lysates of the corresponding 293T transfectants (T). (A) Western blot detection of viral PA (top panel) and M1 (bottom panel) proteins in erythrocyte-adsorbed material. The polyclonal anti-PA antibody used here detects J10 protein when present (Fig. 1B and 5). (B) Detection of NA-specific RNA species by primer extension assay. (C) Detection of viral RNAs by quantitative RT-PCR. Aliquots of RNA from transfected 293T cells (top panel) were treated with DNase and normalized to expression of 5.8S rRNA prior to analysis. RNA from equal volumes of the corresponding supernatants (bottom panel) was analyzed following erythrocyte adsorption and MCN digestion. Segment-specific RT-PCR was performed using vRNA-specific primers for the RT phase. Data are expressed as the number of PCR cycles required to reach C_T, which is inversely proportional to concentration of the target RNA; RNAs from virions and wild-type VLPs were diluted 50-fold for analysis, and their depicted C_T values were adjusted accordingly. The mean difference in C_T values shown here for all eight segments between J10 and WT supernatants corresponds to a 9,400-fold average difference in RNA concentration.

of those proteins was detectable in supernatants from J10 transfectants (J10) or when PA vectors were omitted from the transfection (−PA). As shown in Fig. 7B, a primer extension assay was then used to probe for sequences from the viral NA gene in RNA extracted from the transfected cells (T), as well as from the erythrocyte-adsorbed supernatants both before (−) and after (+) digestion with MCN. Although cells transfected with all 17 WT vectors expressed abundant NA-specific vRNA, mRNA, and cRNA, the adsorbed material from their supernatants contained almost exclusively vRNA that was nuclease resistant and indistinguishable from that found in similarly enriched authentic virions (Vir), implying that it had been packaged selectively into intact VLPs. When PA vectors were omitted (−PA), only the background of vector-derived NA vRNA was expressed in the cells, and none was detected in erythrocyte-adsorbed supernatant. As expected, lysates from J10-transfected cells contained all three forms of viral RNA, confirming that a J10-containing polymerase can both replicate and transcribe a native NA vRNA. Strikingly, however, erythrocyte adsorption failed to recover any detectable NA-specific vRNA. We extended this finding by using a highly sensitive, quantitative RT-PCR assay to search for RNA products of all eight viral segments individually. As shown in Fig. 7C (top panel), an average of four fewer PCR cycles were required to reach critical threshold (C_T) for any segment in wild-type- than in J10-transfected 293T cells (i.e., the C_T value was lower by 4), indicating that wild-type transfectants expressed roughly 16-fold more of the cognate RNA. Parallel assays of hemagglutinated, nuclease-treated supernatants from those cells (Fig. 7C, bottom panel), in comparison, revealed that products of all eight segments were 2,000- to 30,000-fold more abundant in wild-type than in J10 supernatants and were only modestly (i.e., less than 100-fold) more abundant in J10 supernatants than when PA vectors were omitted entirely. Together, these results demonstrate that any hemagglutinating VLPs that may be present in J10 supernatants are essentially devoid of viral RNA.

DISCUSSION

The results of this study add to a growing body of mutational data on the roles of PA in the influenza virus life cycle. In agreement with earlier studies, our analysis of 16 novel substitution mutations in PA reveals a spectrum of effects on polymerase function (Fig. 2). Certain mutations (e.g., J2, J3, J7, J13, and J16) impair the synthesis of all three classes of influenza virus RNA, confirming that PA is essential for polymerase function and for viral infectivity. Some in the latter group (e.g., J3 and J16) map in or near regions that mediate nuclear localization (21) or PB1 binding (22, 26), which likely accounts for their effects. Other mutations (e.g., J8) have subtler consequences, in some cases promoting the accumulation of specific RNA classes at the expense of others. Additional study will be needed to unravel the mechanisms underlying those phenomena, which might reflect activities intrinsic to PA or indirect effects on the function, stability, or localization of the polymerase holoenzyme or of its RNA products (31).

The present study focused principally on the novel phenotype of one mutant, J10, that suggests a previously unrecognized role for PA in influenza virus assembly. In our initial screening, this mutant was found to be unique in its complete failure to produce infectious virus despite its ability to support relatively high-level expression of all three RNA classes. The catalytic integrity of J10-containing polymerase was evident in transfected 293T cells expressing all of the proteins and RNAs necessary for virion assembly (Fig. 4 and 7C), as well as in those expressing only the four viral proteins (PA, PB1, PB2,

and NP) minimally required for polymerase function (Fig. 2). During the course of our study, J10-containing polymerases proved capable of utilizing both vRNA and cRNA templates as well as a variety of vRNA reporters. Although we cannot formally rule out a defect in expressing a subset of viral genes, our results demonstrate that this mutant polymerase can efficiently act on substrate RNAs from the NA (Fig. 2 and 7B), PB2 (Fig. 4), and NS1 (Fig. 5) genes. This functionality implies that J10 does not interfere with polymerase trimer assembly or substrate binding, though experiments to test this directly were not carried out. The various RNA products of J10 polymerase also appeared normal in physical assays such as primer extension (Fig. 2A, 5, and 7B) and by functional criteria. In particular, the ability of J10-containing polymerase to amplify vRNAs (Fig. 2A, B, and E and 7) implies that it synthesizes functional cRNA intermediates, and our studies demonstrate that mRNAs that it produces can be translated to yield luciferase (Fig. 2D) or GFP (Fig. 4 and 5). The levels of J10-dependent protein or RNA expression that we measured were generally at least 50% of the wild-type level and exceeded those observed with certain other PA mutants (e.g., J4 and J12) that supported viral growth and plaque formation. Thus, we found no enzymatic defect in J10-containing polymerase that could account for its profound defect in generating plaque-forming virions.

Instead, the replicative defect of J10 appears to reflect a failure to assemble viable virions. Notwithstanding high-level expression of all requisite virion constituents, J10-transfected 293T cells fail to produce detectable VLPs whose buoyant density approximates that of wild-type influenza virus virions; the relevant glycerol density fractions contained virtually no viral RNA, M1 protein, or plaque-forming activity (Fig. 6). Moreover, although the supernatants from J10 transfectants exhibit substantial hemagglutinating activity (Table 1), implying the release of particles that can bind chicken erythrocytes, we found that enriching for such particles in J10 supernatants yields no detectable nuclease-resistant vRNA, a hallmark of intact virions (Fig. 7).

The J10 mutation alters a potentially surface-exposed glycine-arginine pair at positions 507 and 508 in PA. The functional architecture of this region of PA is unknown, but an earlier study found that single-codon mutations at a cluster of nearby residues (positions 502, 510, 524, and 539) each abolished infectivity (3). The reported effects of those mutations on viral RNA expression varied widely, however, and none recapitulated the phenotype of J10. Interestingly, the normal sequence of residues 502 to 509 resembles a motif called the P loop ([G/A]XXXXGK[S/T]), which functions in other proteins as an ATP- or GTP-binding site (2, 16, 23), though the biological significance of this resemblance remains speculative. Insertion of a serine residue after position 509 has been reported to yield a dominant-negative mutant that inhibits the activity of wild-type PA in *trans* (32).

Our inability to detect production of RNA-containing particles by J10 transfectants is particularly striking in that the influenza virus M1, hemagglutinin, and NA proteins alone can direct formation and release of hemagglutinating VLPs (13, 20). This raises the hypothesis that the J10 mutant either interferes with the production of such VLPs or prevents them from incorporating vRNAs and, perhaps, other key components. Though the potential involvement of PA in influenza virus virion assembly has not been extensively explored, polymerase trimers are known to be contained in the virion core, bound stably to the 3′ and 5′ ends of each vRNA. Electron micrographs of influenza virus cores suggest that the vRNAs within them are packed in a densely stacked array (11, 17), and, while the nature of this array and the factors that give rise to it have not yet been determined, polymerase may conceivably play a structural role in core formation that might be perturbed by the J10 mutation. Alternatively, by virtue of binding to vRNAs, the polymerase might collaborate with other viral or cellular proteins that direct the intracellular trafficking of vRNAs to sites of viral assembly. Indeed, polymerase has been speculated to play a role in the differential cytoplasmic accumulation of vRNA as opposed to cRNA (30). Although our data indicate that both J10 and wild-type PA support cytoplasmic vRNA accumulation (Fig. 5), we cannot rule out subtler localization defects that might result from this mutation. Finally, assuming that all components are present at the assembly sites, one may speculate that PA provides signals that target a polymerase complex into nascent virions, bringing with it a vRNA bound through its PB1 and PB2 subunits. Precedent for this model may be found in the hepatitis B virus, whose polymerase mediates packaging in *trans* when bound to its genomic operator site (27). The loss of PA-associated packaging signals might thus account for the apparent failure of our J10 mutant to incorporate viral RNA into VLPs. If correct, this model would implicate PA as a critical *trans*-acting factor in the pathway of influenza virus vRNA packaging, whose mechanism is currently unknown.

ACKNOWLEDGMENTS

We thank C. T. Bancroft, J. Clever, A. Tward, I. Hsieh, S. Johns, L. Tiley, and N. Naffakh for helpful discussions and advice; J. McKerrow for laboratory space; T. Toyoda for anti-PA antiserum used in pilot studies; and H. Ly for comments on the manuscript.

This work was supported by NIH grants AI-36636 and AI-40317.

REFERENCES

1. **Bancroft, C. T., and T. G. Parslow.** 2002. Evidence for segment-nonspecific packaging of the influenza A virus genome. J. Virol. **76:**7133–7139.
2. **Delaluna, S., C. Martinez, and J. Ortin.** 1989. Molecular cloning and sequencing of influenza virus A/Victoria/3/75 polymerase genes—sequence evolution and prediction of possible functional domains. Virus Res. **13:**143–156.
3. **Fodor, E., M. Crow, L. J. Mingay, T. Deng, J. Sharps, P. Fechter, and G. G. Brownlee.** 2002. A single amino acid mutation in the PA subunit of the influenza virus RNA polymerase inhibits endonucleolytic cleavage of capped RNAs. J. Virol. **76:**8989–9001.
4. **Fodor, E., L. J. Mingay, M. Crow, T. Deng, and G. G. Brownlee.** 2003. A single amino acid mutation in the PA subunit of the influenza virus RNA polymerase promotes the generation of defective interfering RNAs. J. Virol. **77:**5017–5020.
5. **Gomez-Puertas, P., C. Albo, E. Perez-Pastrana, A. Vivo, and A. Portela.** 2000. Influenza virus matrix protein is the major driving force in virus budding. J. Virol. **74:**11538–11547.
6. **Greenspan, D., P. Palese, and M. Krystal.** 1988. Two nuclear location signals in the influenza virus NS1 nonstructural protein. J. Virol. **62:**3020–3026.
7. **Hara, K., M. Shiota, H. Kido, Y. Ohtsu, T. Kashiwagi, J. Iwahashi, N. Hamada, K. Mizoue, N. Tsumura, H. Kato, and T. Toyoda.** 2001. Influenza virus RNA polymerase PA subunit is a novel serine protease with Ser624 at the active site. Genes Cells **6:**87–97.
8. **Hoffmann, E., G. Neumann, Y. Kawaoka, G. Hobom, and R. G. Webster.** 2000. A DNA transfection system for generation of influenza A virus from eight plasmids. Proc. Natl. Acad. Sci. USA **97:**6108–6113.
9. **Huarte, M., A. Falcon, Y. Nakaya, J. Ortin, A. Garcia-Sastre, and A. Nieto.** 2003. Threonine 157 of influenza virus PA polymerase subunit modulates RNA replication in infectious viruses. J. Virol. **77:**6007–6013.

10. **Kawaguchi, A., T. Naito, and K. Nagata.** 2005. Involvement of influenza virus PA subunit in assembly of functional RNA polymerase complexes. J. Virol. **79:**732–744.
11. **Knipe, D. M., B. N. Fields, P. M. Howley, and D. E. Griffin.** 2001. Fields virology, 4th ed. Lippincott Williams & Wilkins, Philadelphia, Pa.
12. **Krug, R. M., M. Ueda, and P. Palese.** 1975. Temperature-sensitive mutants of influenza WSN virus defective in virus-specific RNA synthesis. J. Virol. **16:**790–796.
13. **Latham, T., and J. M. Galarza.** 2001. Formation of wild-type and chimeric influenza virus-like particles following simultaneous expression of only four structural proteins. J. Virol. **75:**6154–6165.
14. **Li, Y., Y. Yamakita, and R. M. Krug.** 1998. Regulation of a nuclear export signal by an adjacent inhibitory sequence: the effector domain of the influenza virus NS1 protein. Proc. Natl. Acad. Sci. USA **95:**4864–4869.
15. **Liang, Y., Y. Hong, and T. G. Parslow.** 2005. *cis*-Acting packaging signals in the influenza virus PB1, PB2, and PA genomic RNA segments. J. Virol. **79:**10348–10355.
16. **Moller, W., and R. Amons.** 1985. Phosphate-binding sequences in nucleotide-binding proteins. FEBS Lett. **186:**1–7.
17. **Murti, K. G., W. J. Bean, Jr., and R. G. Webster.** 1980. Helical ribonucleoproteins of influenza virus: an electron microscopic analysis. Virology **104:** 224–229.
18. **Naffakh, N., P. Massin, and S. van der Werf.** 2001. The transcription/replication activity of the polymerase of influenza A viruses is not correlated with the level of proteolysis induced by the PA subunit. Virology **285:**244–252.
19. **Neumann, G., T. Watanabe, H. Ito, S. Watanabe, H. Goto, P. Gao, M. Hughes, D. R. Perez, R. Donis, E. Hoffmann, G. Hobom, and Y. Kawaoka.** 1999. Generation of influenza A viruses entirely from cloned cDNAs. Proc. Natl. Acad. Sci. USA **96:**9345–9350.
20. **Neumann, G., T. Watanabe, and Y. Kawaoka.** 2000. Plasmid-driven formation of influenza virus-like particles. J. Virol. **74:**547–551.
21. **Nieto, A., S. de la Luna, J. Barcena, A. Portela, and J. Ortin.** 1994. Complex structure of the nuclear translocation signal of influenza virus polymerase PA subunit. J. Gen. Virol. **75:**29–36.
22. **Ohtsu, Y., Y. Honda, Y. Sakata, H. Kato, and T. Toyoda.** 2002. Fine mapping of the subunit binding sites of influenza virus RNA polymerase. Microbiol. Immunol. **46:**167–175.
23. **Paez, J. G., P. A. Janne, J. C. Lee, S. Tracy, H. Greulich, S. Gabriel, P. Herman, F. J. Kaye, N. Lindeman, T. J. Boggon, K. Naoki, H. Sasaki, Y. Fujii, M. J. Eck, W. R. Sellers, B. E. Johnson, and M. Meyerson.** 2004. EGFR mutations in lung cancer: correlation with clinical response to gefitinib therapy. Science **304:**1497–1500.
24. **Parvin, J. D., P. Palese, A. Honda, A. Ishihama, and M. Krystal.** 1989. Promoter analysis of influenza virus RNA polymerase. J. Virol. **63:**5142–5152.
25. **Perales, B., J. J. Sanz-Ezquerro, P. Gastaminza, J. Ortega, J. F. Santaren, J. Ortin, and A. Nieto.** 2000. The replication activity of influenza virus polymerase is linked to the capacity of the PA subunit to induce proteolysis. J. Virol. **74:**1307–1312.
26. **Perez, D. R., and R. O. Donis.** 2001. Functional analysis of PA binding by influenza A virus PB1: effects on polymerase activity and viral infectivity. J. Virol. **75:**8127–8136.
27. **Pollack, J. R., and D. Ganem.** 1994. Site-specific RNA binding by a hepatitis B virus reverse transcriptase initiates two distinct reactions: RNA packaging and DNA synthesis. J. Virol. **68:**5579–5587.
28. **Ruigrok, R. W., and F. Baudin.** 1995. Structure of influenza virus ribonucleoprotein particles. II. Purified RNA-free influenza virus ribonucleoprotein forms structures that are indistinguishable from the intact influenza virus ribonucleoprotein particles. J. Gen. Virol. **76:**1009–1014.
29. **Sanz-Ezquerro, J. J., T. Zurcher, S. de la Luna, J. Ortin, and A. Nieto.** 1996. The amino-terminal one-third of the influenza virus PA protein is responsible for the induction of proteolysis. J. Virol. **70:**1905–1911.
30. **Tchatalbachev, S., R. Flick, and G. Hobom.** 2001. The packaging signal of influenza viral RNA molecules. RNA **7:**979–989.
31. **Vreede, F. T., T. E. Jung, and G. G. Brownlee.** 2004. Model suggesting that replication of influenza virus is regulated by stabilization of replicative intermediates. J. Virol. **78:**9568–9572.
32. **Zurcher, T., S. de la Luna, J. J. Sanz-Ezquerro, A. Nieto, and J. Ortin.** 1996. Mutational analysis of the influenza virus A/Victoria/3/75 PA protein: studies of interaction with PB1 protein and identification of a dominant negative mutant. J. Gen. Virol. **77:**1745–1749.